

# Precipitation processes in Cu-Co-Si alloys

J. LENDVAI, T. UNGÁR, I. KOVÁCS

*Institute for General Physics, Eötvös University, Budapest, Hungary*

B. ALBERT

*Csepel Metal-Works, Budapest, Hungary*

The precipitation of cobalt and silicon atoms from supersaturated solid solutions of Cu-Co-Si alloys was studied during ageing between 400 and 600° C by electrical resistivity, thermoelectric power and calorimetric measurements, by mechanical testing and by transmission electron microscopy investigations. It has been found that the decomposition begins with the appearance of concentration fluctuations from which cobalt precipitates first. The clustering of cobalt atoms initiates the precipitation of silicon, and so particles with the stoichiometric  $\text{Co}_2\text{Si}$  composition are finally formed. The silicon that is in excess with respect to the stoichiometry of  $\text{Co}_2\text{Si}$  is retained in the solid solution but its increase in the initial supersaturated solid solution strongly enhances the nucleation of the particles and, therefore, results in a finer precipitate structure. On the basis of calorimetric measurements the effective activation energy of both the cobalt and silicon precipitation was determined to be around 1.5 eV.

## 1. Introduction

Since the early work of Corson [1] the precipitation processes and the precipitation hardening in Cu-Co-Si alloys have been investigated by several authors [2-8]. It is now well established that the orthorhombic  $\text{Co}_2\text{Si}$  phase is the equilibrium precipitate phase [1-3, 5, 6, 9]. Recently the solid solubilities of cobalt and silicon in the presence of  $\text{Co}_2\text{Si}$  precipitates have also been investigated [10].

In this paper we report on investigations carried out on a series of Cu-Co-Si alloys containing approximately the same amount of cobalt but various amounts of surplus silicon with respect to the stoichiometric  $\text{Co}_2\text{Si}$  composition. By applying the simultaneous measurements of electrical resistivity and thermoelectric power, supplemented by calorimetric and TEM investigations, we aim at conclusions concerning the early stages of the decomposition during ageing at temperatures between 400 and 600° C.

## 2. Experimental procedure

The composition of the alloys investigated is listed in Table I. The alloys were prepared from 99.99% purity cathode copper and 99.99% purity cobalt and silicon in an induction furnace. The cast ingots were homogenized for 6 h at 900° C and subsequently hot-forged to 15 mm diameter rods. After pickling the rods were drawn to 6 mm diameter, then annealed for 10 min at 800° C, pickled again and drawn to 1.5 mm diameter wires. With the exception of transmission electron microscopy (TEM) investigations all measurements were carried out on these wire samples. The TEM samples were obtained by cold-rolling the 1.5 mm wires to plates of 0.3 mm thickness.

The samples were heat-treated in a vacuum better than 0.01 Pa. For solution treatment the specimens

were kept for 1 h at 1000° C and subsequently quenched in room-temperature silicon oil. The measurement of the electrical resistivity and of the thermoelectric power (TEP) against high-purity copper was carried out at 25° C. The theoretical basis of the evaluation and the experimental details of these measurements were described previously [8].

For TEM experiments the samples were double-jet thinned in a Struers Tenupol apparatus at -30° C and investigated in a Tesla BS 540 electron microscope operated at 120 kV.

Calorimetric measurements were carried out in a Perkin-Elmer DSC-2 microcalorimeter. High-purity dry nitrogen was used as purge gas.

The mechanical properties of the samples were tested by simultaneous torsion and extension. The tests were performed at 78 K in liquid nitrogen. The strain rate was  $2 \times 10^{-3} \text{ sec}^{-1}$ . The torsional flow stress,  $\tau_f$ , was determined from the measured value of the applied torque according to the method of Nádai [11]. More details of the method have been described elsewhere [12].

## 3. Results and discussion

### 3.1. Transport measurements

The changes in the solute cobalt and silicon concentrations were followed by simultaneous measurement of the electrical resistivity and thermoelectric power in the course of heat treatments at 400, 500 and 600° C after solution treatment and quenching. The time of heat treatment was varied between zero and 4 h. The Nordheim-Gorter (NG),  $\rho\Delta S$  against  $\Delta\rho$  diagrams are shown in Fig. 1. The NG diagrams corresponding to the four alloys of different composition are very similar; with increasing silicon content the curves are shifted to the right. The upper end of each curve

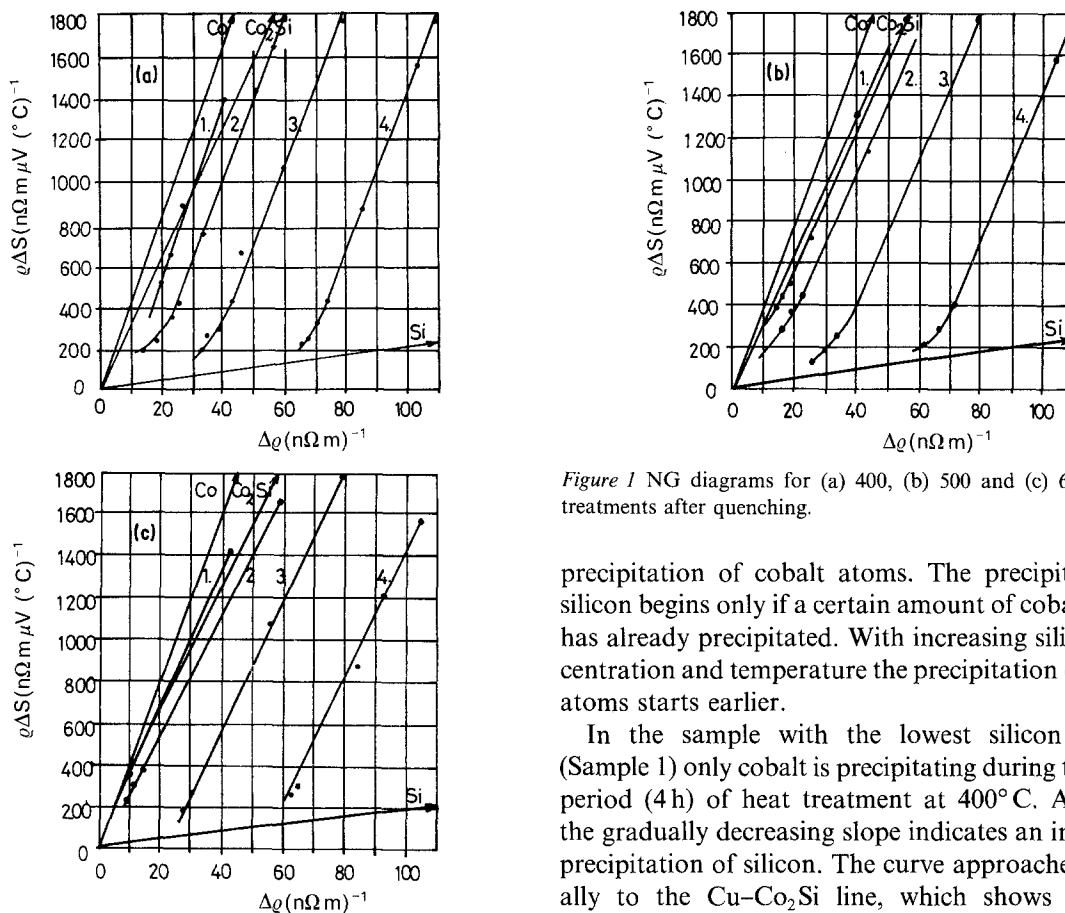


Figure 1 NG diagrams for (a) 400, (b) 500 and (c) 600°C heat treatments after quenching.

corresponds to the as-quenched state of the sample, and the curves progressing downwards characterize the changes of solute concentration in the sample. The binary Cu-Co and Cu-Si as well as the quasi-binary Cu-Co<sub>2</sub>Si lines have also been included in the figure. If the NG diagram of a given ternary alloy is running parallel to one of the Cu-Co or Cu-Si straight lines it indicates that only the solute cobalt or the solute silicon concentration is decreasing in the sample, i.e. cobalt- or silicon-containing particles are being formed, respectively. In like manner, if a part of an NG curve runs parallel to the Cu-Co<sub>2</sub>Si line it shows that Co<sub>2</sub>Si particles are precipitating from the supersaturated solid solution.

At 400°C the initial parts of the NG curves are linear and parallel to the Cu-Co line, indicating that the decomposition starts with the precipitation of cobalt. Following this linear part the curves deviate from the straight line; their slope decreases gradually and approximates that of the Cu-Si line. The slope of the initial linear part decreases with increasing temperature of heat-treatment at 500°C the slopes are between the slopes of the Cu-Si and Cu-Co<sub>2</sub>Si lines, while at 600°C the curves run parallel to the Cu-Co<sub>2</sub>Si line. The fact that the initial slopes are between the slopes of the Cu-Co and Cu-Co<sub>2</sub>Si lines suggests that decomposition always starts with the

precipitation of cobalt atoms. The precipitation of silicon begins only if a certain amount of cobalt atoms has already precipitated. With increasing silicon concentration and temperature the precipitation of silicon atoms starts earlier.

In the sample with the lowest silicon content (Sample 1) only cobalt is precipitating during the entire period (4 h) of heat treatment at 400°C. At 500°C the gradually decreasing slope indicates an increasing precipitation of silicon. The curve approaches gradually to the Cu-Co<sub>2</sub>Si line, which shows that the composition of the precipitates approaches to the stoichiometric Co<sub>2</sub>Si composition. At 600°C the Co<sub>2</sub>Si composition of the precipitates develops very soon at the beginning of the heat treatment, and the growth of the particles proceeds corresponding to the Co<sub>2</sub>Si stoichiometry.

The NG curves of the samples with larger silicon content are shifted systematically to the right. This indicates that only the amount of silicon necessary to attain the Co<sub>2</sub>Si composition in the particles precipitates, and the excess silicon is kept dissolved. This is supported by the fact that the intersections of the linear parts of the NG curves with the  $\Delta q$  axis are in a linear relation with the silicon concentration of the samples. With increasing silicon content both the rate and the extent of the precipitation is increased; consequently in the samples with higher silicon concentration the precipitation of silicon can already be observed at 400°C, while at 500°C the Co<sub>2</sub>Si phase is already being formed.

### 3.2. TEM investigations

In Figs 2 and 3 TEM micrographs of Samples 1 and 2 are shown for different heat treatments. During 30 min at 500°C a homogeneous precipitate structure is formed in both samples. This modulated structure is probably formed by spatial concentration fluctuations. The wavelength of the concentration fluctuations is between 20 and 50 nm, the lower value being characteristic of the sample with higher silicon concentration.

With longer heat treatments at 500°C (Figs 2b and 3b) the precipitate particles become definitely separated from the matrix. The average particle size is 5 to 10 nm and the average interparticle distance is 20 to 50 nm, which is equal to the wavelength of the

TABLE I Alloy composition

Sample No.	Co (at %)	Si (at %)
1	0.63	0.27
2	0.64	0.48
3	0.67	1.02
4	0.56	1.91

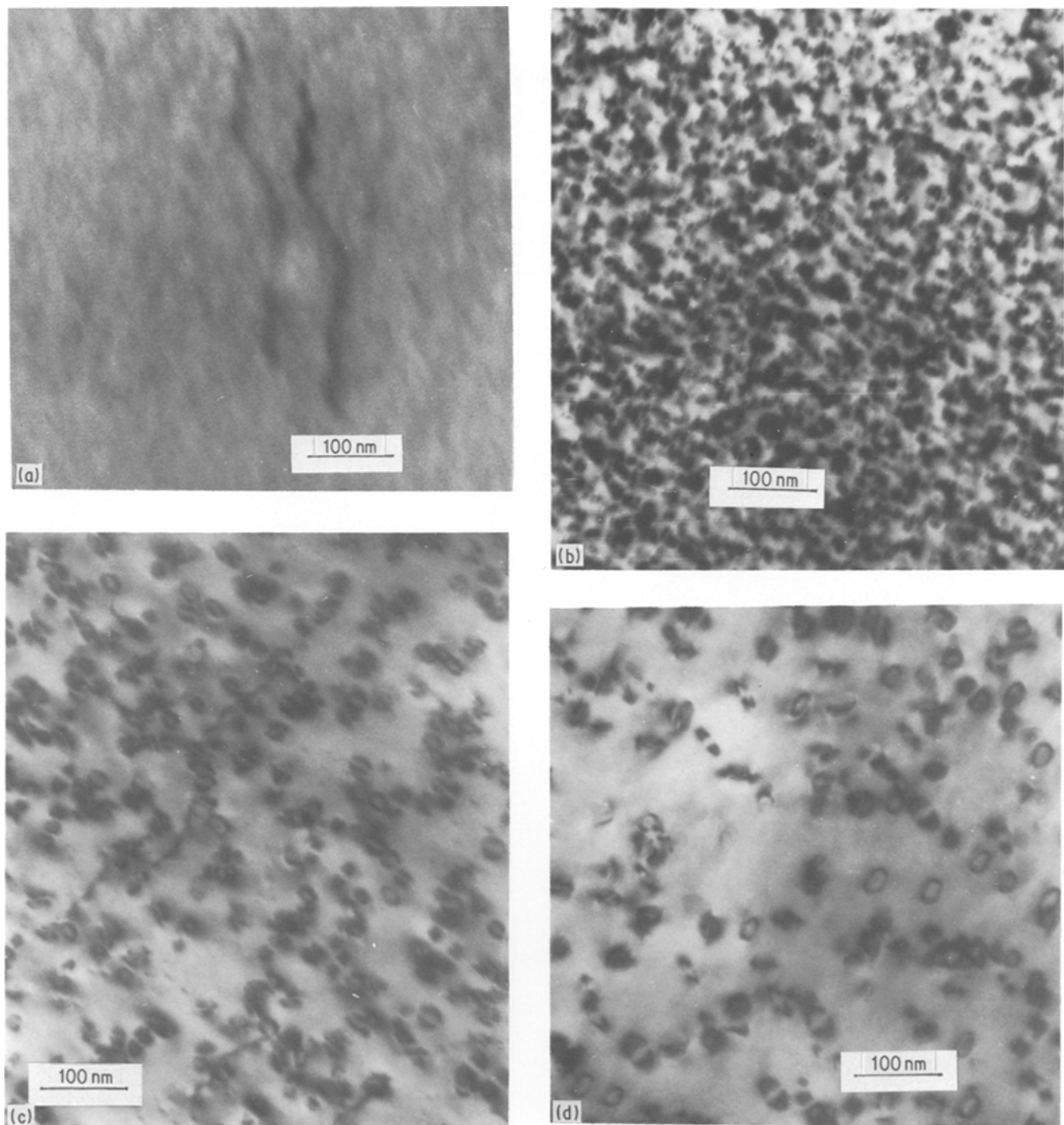


Figure 2 TEM micrographs of Sample 1 after different heat treatments: (a) 500° C, 30 min; (b) 500° C, 8 h; (c) 600° C, 20 min and (d) 600° C, 2 h.

concentration fluctuations observed after the shorter heat treatment. On the basis of this observation it can be concluded that the precipitates are nucleated on the higher-concentration regions of the original modulated structure.

At 600° C the precipitates can be clearly observed already after 20 min of heat treatment (Figs 2c and 3c). In the sample with higher silicon content (Sample 2) the average particle size and interparticle distance are significantly smaller than in Sample 1 and the distribution of the precipitates is more homogeneous. The characteristic coffee-bean outline of the particles indicates the presence of coherency strains. In course of further heat treatment at 600° C the particle size increases while the dispersity of the precipitate structure decreases (Figs 2d and 3d). The changes are particularly strong in the case of Sample 2. These results show that particle coarsening and over-aging

starts very soon at 600° C. In the case of Sample 1, dislocation loops are observed around certain particles indicating the beginning of the transition from full to partial coherency.

### 3.3. Mechanical measurements

The changes of the yield stress of Samples 1 and 2 obtained by torsion tests are shown in Fig. 4. The yield stress of Sample 1 is monotonously increases during ageing at 500° C; it is constant after ageing between 20 min and 2 h at 600° C and then it slightly decreases. In agreement with the transport investigations, the results of the torsion tests also reveal the enhancement of the precipitation process in consequence of the excess silicon content in Sample 2. At 500° C the yield stress of Sample 2 increases strongly up to 2 h of heat treatment and it remains unchanged thereafter. A 2 h ageing at 500° C of Sample 2 is sufficient to attain

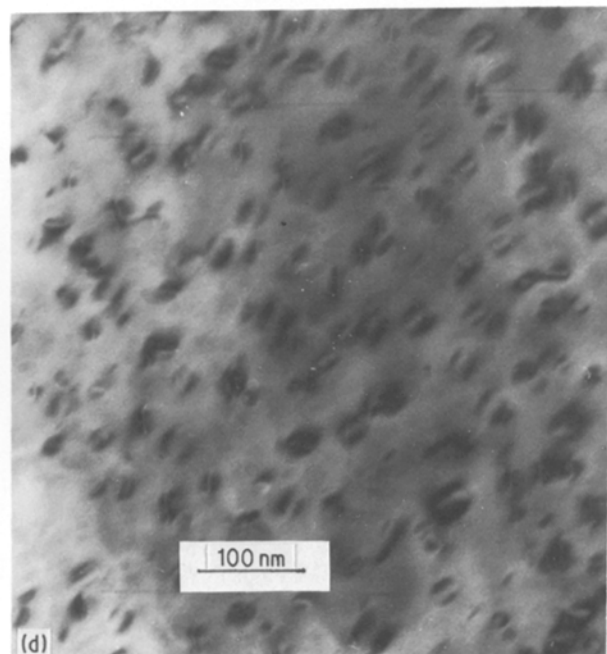
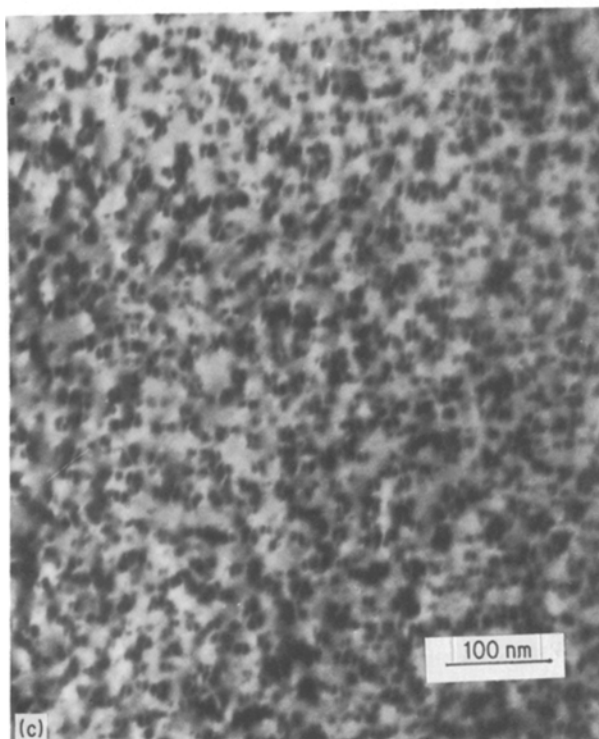
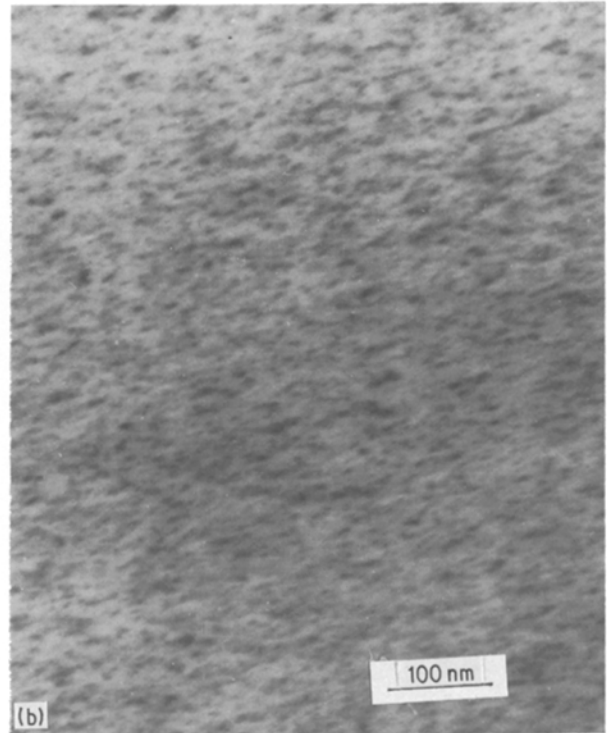
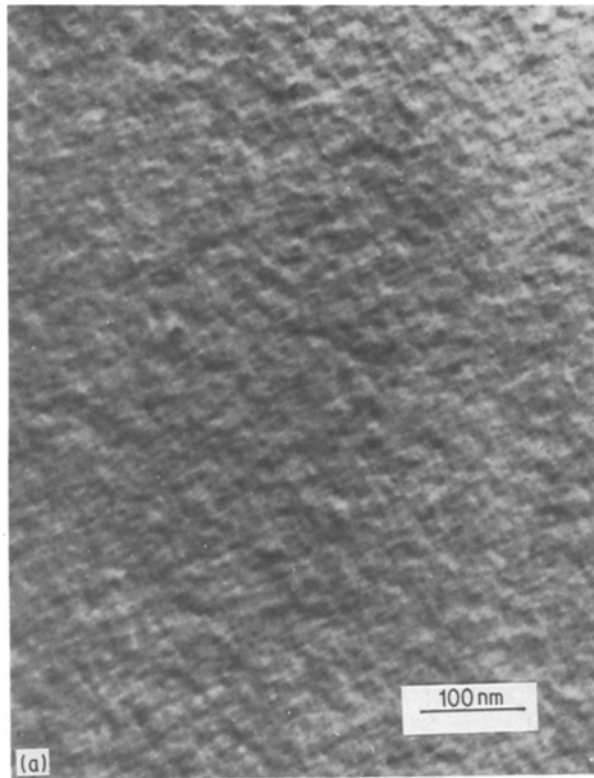


Figure 3 The same as in Fig. 2, for Sample 2.

the same increase in yield stress as that produced by 8 h heat treatment in Sample 1. The yield stress of Sample 2 increases very rapidly at the beginning of the ageing at 600°C, and 20 min ageing already leads to over-ageing in agreement with the results of the TEM investigations.

### 3.4. Calorimetry

In Fig. 5, differential scanning calorimetry (DSC) thermograms obtained at 10, 20 and 40°C min<sup>-1</sup> constant heating rates on quenched samples are shown. The thermograms of Sample 1 (Fig. 5a) reveal

two distinct exothermal peaks which become more and more overlapping in the case of the other alloys with increasing silicon content. Taking into account the results of the transport measurements, the two peaks can be associated with the formation of cobalt and Co<sub>2</sub>Si precipitates, respectively. The temperature ranges of the peaks are shifted to lower temperatures with increasing silicon concentration. To illustrate this tendency, in Fig. 6 the peak temperatures of the two exothermal reactions – cobalt and Co<sub>2</sub>Si precipitation – are plotted against the silicon content in the samples, the cobalt concentrations being approximately

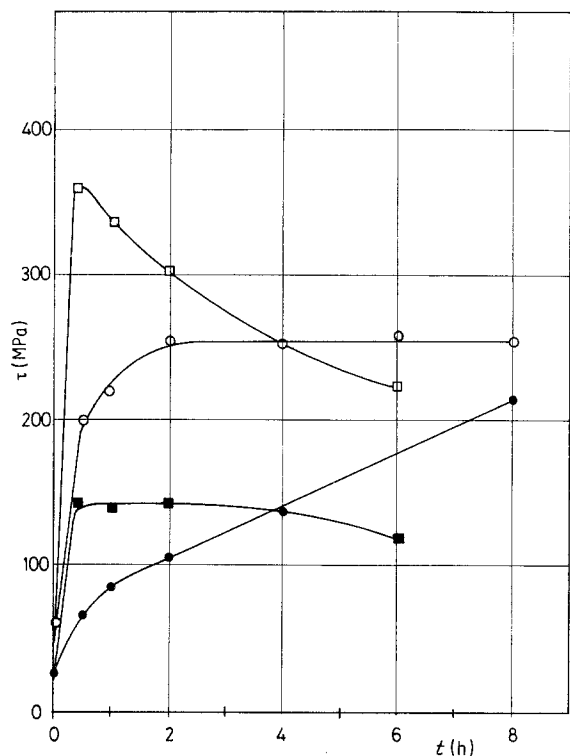


Figure 4 The changes in the torsional yield stress of Samples 1 and 2 upon 500 and 600°C heat treatments: (●) Sample 1, 500°C; (■) Sample 1, 600°C; (○) Sample 2, 500°C; (□) Sample 2, 600°C.

constant. In the case of cobalt precipitation (Fig. 6a) the decrease in the peak temperature is rather small, while the effect is much more pronounced in the case of the  $\text{Co}_2\text{Si}$  formation (Fig. 6b). The same influence of increasing silicon concentration on the precipitation process was revealed also by the transport measurements. In consequence of the more significant

decrease in the temperature range of  $\text{Co}_2\text{Si}$  formation, the two exothermal peaks observed in the thermograms become increasingly overlapping with higher silicon content.

In the case of the sample with the highest silicon content (Sample 4), in addition to the strongly overlapping cobalt and  $\text{Co}_2\text{Si}$  peaks, at somewhat higher temperatures (about 550°C) a third exothermal peak is also observed in the thermograms (Fig. 5d) which appears most markedly in the  $10^\circ\text{C min}^{-1}$  thermogram. With increasing heating rate the area of this peak, and correspondingly the reaction heat of this process, is strongly decreasing. Since this third exothermal peak was observed only in the alloy with the highest silicon content it is probably connected with the precipitation of silicon.

On the basis of the thermograms obtained by constant heating-rate measurements the effective activation energies of the processes can be determined either from the Kissinger equation [13]:

$$\ln \frac{v}{T_m^2} = \frac{E}{k} \left( \frac{1}{T_m} \right) + \ln \frac{vk}{E} \quad (1)$$

or from the Ozawa equation [14, 15]:

$$\ln v = -1.052 \frac{E}{k} \left( \frac{1}{T_m} \right) + \ln (vT_m) \quad (2)$$

which differ only slightly from each other in the approximations applied. Here  $v$  is the constant heating rate,  $E$  the activation energy,  $k$  the Boltzmann factor,  $T_m$  the peak temperature and  $v$  the frequency factor. From the thermograms in Fig. 5 the activation energy of the first reaction (cobalt precipitation) was determined as  $1.40 \pm 0.1 \text{ eV}$ , while for the second peak ( $\text{Co}_2\text{Si}$  precipitation)  $1.53 \pm 0.1 \text{ eV}$  was obtained.

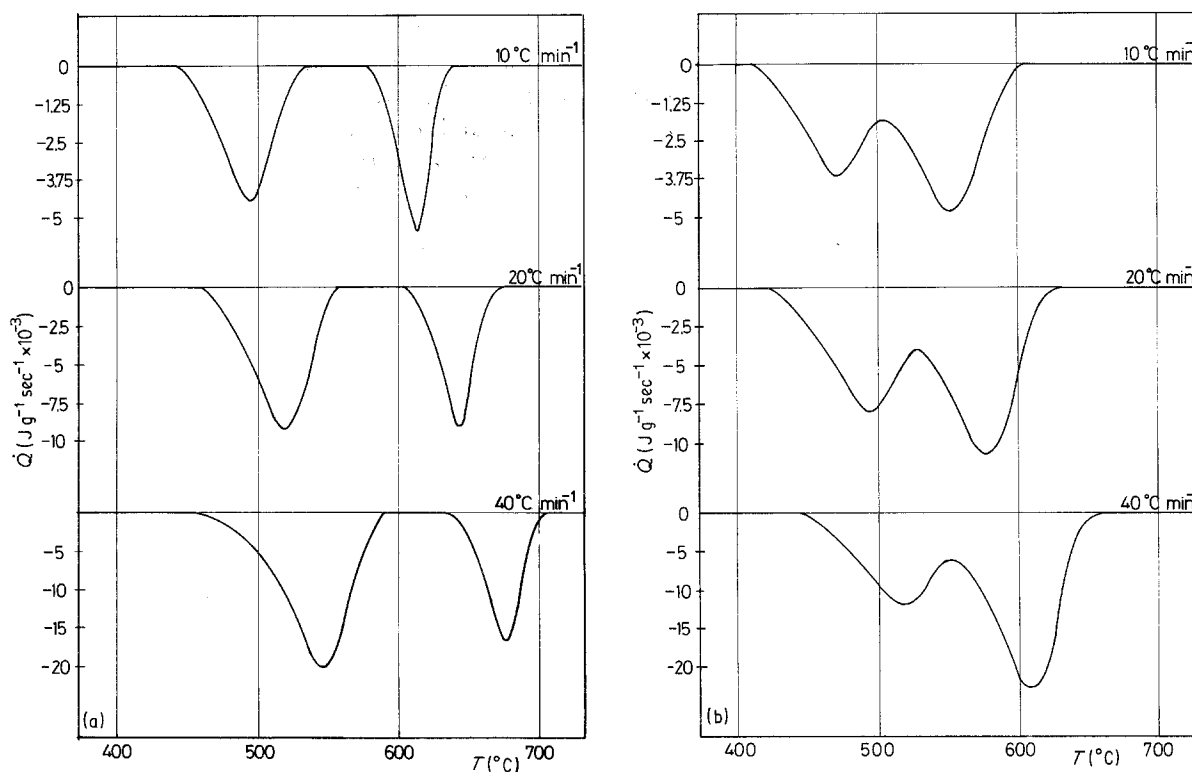


Figure 5 DSC thermograms measured by different heating rates on quenched samples: (a) Sample 1, (b) Sample 2, (c) Sample 3, (d) Sample 4.

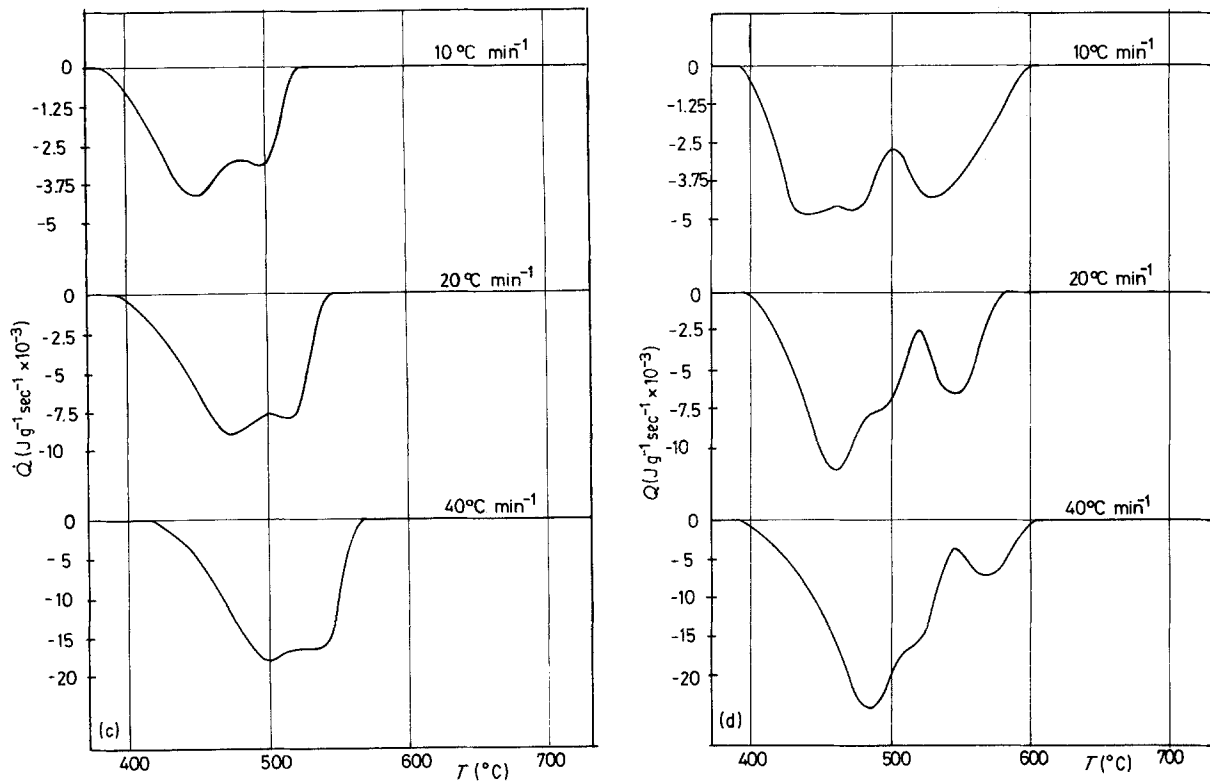


Figure 5 Continued.

Within the accuracy of the determination these activation energies were found to be independent of the silicon content in the alloys investigated. The activation energy due to the third peak observed in the alloy with the highest silicon content is  $2.0 \pm 0.15$  eV.

#### 4. Summary and conclusion

In the Cu-Co-Si alloys investigated the decomposition of the supersaturated solid solution obtained by solution treatment and quenching starts with the precipitation of cobalt atoms. The precipitation of cobalt initiates the precipitation of silicon atoms during ageing, even at those silicon concentrations which remain in solid solution in the binary Cu-Si system.

At the beginning of the 400 and 500°C heat treat-

ments, homogeneously distributed fully coherent cobalt-containing particles are formed at the high-concentration sites of concentration fluctuations which develop at the very early stages of the process. The coherency is retained even in the course of long-term (8 h) heat treatments at 500°C. At 600°C, on the other hand, concentration fluctuations could not be detected. TEM micrographs reveal precipitates separated by definite interfaces from the matrix already after 20 min heat treatment at 600°C. The particles, however, remain coherent with the matrix even in the stage of particle coarsening as demonstrated by the stress contrasts in the TEM pictures (Figs 2d and 3d), although after about 2 h ageing at 600°C the transformation from the fully to the partially coherent structure sets in, which is evidenced by

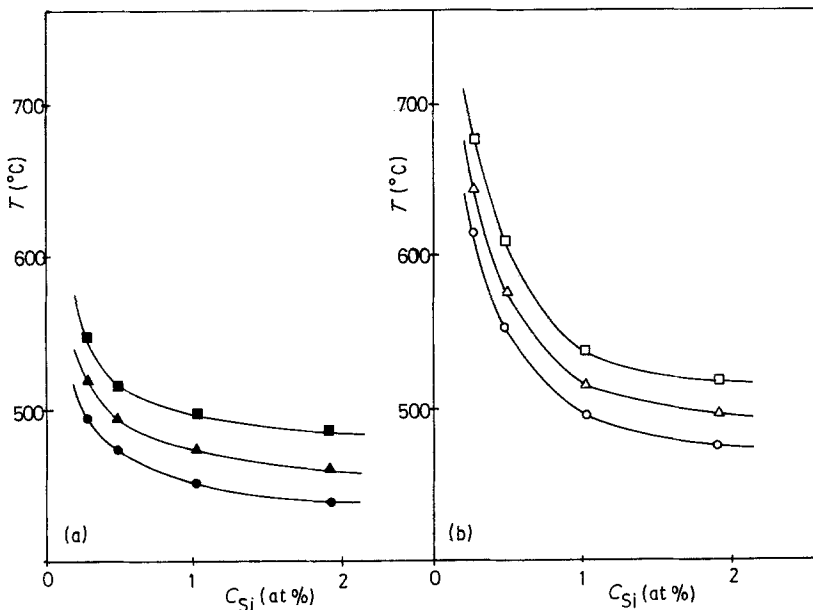


Figure 6 Peak temperatures of the exothermal reactions in Fig. 5 against the silicon content of the samples: (a) first reaction (cobalt precipitation), (b) second reaction ( $\text{Co}_2\text{Si}$  formation). ( $\bullet$ ,  $\circ$ )  $10^\circ\text{C min}^{-1}$ ; ( $\blacktriangle$ ,  $\triangle$ )  $20^\circ\text{C min}^{-1}$ ; ( $\blacksquare$ ,  $\square$ )  $40^\circ\text{C min}^{-1}$ .

the appearance of dislocation loops around some of the particles (Fig. 2d).

In the alloys containing silicon in excess to the stoichiometric  $\text{Co}_2\text{Si}$  composition the precipitates are more dispersely distributed and the process of decomposition is strongly enhanced, in spite of the fact that the silicon atoms do not take part in the precipitation in the beginning of the process. It appears that silicon atoms retained in solution increase the supersaturation of the solid solution, and lead therefore to a decrease in the critical size of the nuclei and to an increase in the reaction rate and dispersity of the precipitate structure.

### Acknowledgement

The authors are grateful to Drs G. Honyek and L. S. Tóth for making the calorimetric and mechanical measurements.

### References

1. M. G. CORSON, *Rev. Metallurgia* **27** (1930) 265.
2. S. GALLO, *Met. Italiana* **50** (1958) 15.

3. N. I. REVINA, A. K. NIKOLAIEV and V. M. ROSENBERG, *Metalli* **17** (1975) 215.
4. V. F. GRABIN and U. B. MALEVSKY, *Metalloved. i Term. Obrabotka Metallov* **3** (1965) 28.
5. T. TODA, *Trans. Jpn. Inst. Metals* **11** (1970) 24.
6. M. D. TEPLITSKY, A. K. NIKOLAIEV, N. I. REVINA and V. M. ROSENBERG, *Fizika Met. Metalloved.* **40** (1975) 1240.
7. A. KORBEL, W. BOCHNIAK, A. PAWELEK, F. DOBRZANSKI and H. DYBIEC, *Rudy i Metale Niezelarne* **25** (1980) 431.
8. B. ALBERT, *Z. Metallkde* **76** (1985) 528.
9. T. TODA and H. TAKEUCHI, *J. Jpn. Inst. Metals* **11** (1970) 24.
10. B. ALBERT, *Z. Metallkde* **76** (1985) 475.
11. A. NÁDAI, "Theory of Flow and Fracture" (McGraw-Hill, New York, 1956) p. 349.
12. L. S. TÓTH and I. KOVÁCS, *J. Mater. Sci.* **17** (1982) 43.
13. H. E. KISSINGER, *Anal. Chem.* **29** (1957) 1702.
14. T. OZAWA, *J. Thermal Anal.* **2** (1970) 301.
15. *Idem, ibid.* **9** (1976) 369.

*Received 6 September  
and accepted 1 December 1987*